Reviews

STM Investigations of Organic Molecules Physisorbed at the Liquid−Solid Interface

Donna M. Cyr,† Bhawani Venkataraman, and George W. Flynn*

Chemistry Department and Columbia Radiation Laboratory, Columbia University, New York, New York 10027

Received February 1, 1996. Revised Manuscript Received June 11, 1996⊗

Investigations of long-chain hydrocarbon and substituted hydrocarbon materials physisorbed at the liquid−solid interface have provided a particularly fruitful area of investigation for the scanning tunneling microscope (STM). Studies of this kind provide considerable information concerning surface−adsorbate interactions, the nature of the STM contrast mechanism for molecules adsorbed on surfaces, the effect of the chemical nature of the liquid solvent on the rearrangement and bonding of adsorbates, and the role played by the underlying structure of the surface itself (defects, domains, etc.) in determining the molecular arrangement of these adsorbates. All of these studies are aimed at the elucidation and control of surface and adsorbate structures and their relationship to the electronic and chemical properties of materials. The successful imaging of numerous physisorbed organic films at the solution−solid interface has demonstrated that the STM is sensitive enough to differentiate chemical functional groups within these films, but participation of molecular states in the tunneling process for many organic thin-film insulators remains a topic of vigorous discussion. Simulations of the self-assembly of long-chain molecules at the liquid−solid interface provide a microscopic, molecular scale view of the dynamic processes that lead to the kinds of structures observed in STM studies of interfaces. These model molecular dynamics simulations offer useful clues to the physical and chemical driving forces that control molecular assembly. This paper reviews the progress and interconnections among the areas of interfacial adsorbate images, imaging mechanisms, and dynamical processes at the liquid−solid interface.

I. Introduction

The scanning tunneling microscope (STM) has proven to be a remarkable tool for studying surface features and surface electronic structure as well as changes in these features due to chemical reactions. The STM is a very versatile instrument as images can be taken under ultrahigh-vacuum conditions, in air, under liquids (both conducting and insulating), and over a wide temperature range. The original objective of the STM was to image structural and electronic properties of surfaces.[1−4] More recently a number of attempts have been made to image molecules and aggregates which are either adsorbed on or bonded to well-characterized surfaces. Clearly this particular use of the STM is in its earliest stages but holds tremendous potential for the characterization of the structure and properties of polymers on surfaces and a number of other chemically important species. In this regard STM is an analytical tool with the kind of potential exhibited by nuclear magnetic resonance techniques in the 1950s. Although the early chemical uses of NMR were quite rudimentary, the potential for a significant impact on chemical research problems was recognized by a number of workers in the field. For STM to achieve the kind of general applicability to chemical problems now enjoyed by NMR techniques, it will be necessary to develop simple methods for imaging molecules on surfaces in air and to identify physical and chemical properties to which the STM is sensitive. In this regard STM investigations of molecules physisorbed on surfaces provide a general approach toward the application of this technique to the study of the structure, functionality, and aggregation of a wide variety of both conducting and insulating molecules.

Scanning tunneling microscopy has already been successful in identifying important structural and dynamical properties for a number of thin polymer films, molecular adsorbates, and self-assembled monolayers. These studies are of importance in the development of the next generation of electronic and optoelectronic devices, which will require molecular films with very specific mechanical and electronic properties.

Investigations of long-chain hydrocarbon and substituted hydrocarbon materials physisorbed on surfaces but with liquid solvent above the adsorbate have provided a particularly fruitful area of investigation for the STM. Typically these molecules are much shorter than polymers but are easily long enough to provide a picture of many of the forces which control the arrange-

† Marie Curie Postdoctoral Fellow, American Association of University Women.

* To whom correspondence should be addressed.

⊗ Abstract published in *Advance ACS Abstracts,* August 1, 1996.

S0897-4756(96)00113-5 CCC: $12.00

ment and structure of intermediate size molecules on surfaces. Studies of this kind are expected to provide considerable information concerning surface−adsorbate interactions, the nature of the STM contrast mechanism for molecules adsorbed on surfaces, the effect of the chemical nature of the liquid solvent on the arrangement and bonding of adsorbates, and the role played by the underlying structure of the surface itself (defects, domains, etc.) in determining the molecular arrangement of these adsorbates. All of these studies are aimed at the elucidation and control of surface and adsorbate structures and their relationship to the electronic and chemical properties of materials.

II. STM Studies of the Liquid−Solid Interface

One of the first molecules physisorbed on a surface to be imaged with the STM was the liquid crystal, 4-*n*-octyl-4′-cyanobiphenyl (8CB) physisorbed onto the basal plane of graphite.[5−11] The STM images reveal a highly ordered arrangement of molecules on the surface as might be expected for a liquid crystal. High-resolution images of individual molecules show sufficient detail to resolve the aromatic and aliphatic parts of the molecules and even the cyano group, as well as to obtain details of molecular packing and orientation on the surface.

In addition to liquid crystals, molecular adsorbates such as polypeptides,[12,13] nucleic acids,[14] and chiral ferroelectric crystals[15,16] have been imaged as thin films by the STM. Conducting polymers have also been imaged as films, though often these systems are conductive enough to be imaged directly.[17−25] The present review is limited to STM studies of the liquid−solid interface, i.e., systems where the STM images are obtained under a liquid drop and the molecules are physisorbed onto the underlying conducting substrate. Work reviewed here focuses on studies performed since the comprehensive survey by Frommer.[26]

II.A. Solvent and Adsorbate Properties for STM Imaging at the Liquid−Solid Interface. There have been a number of studies of the liquid−solid interface where STM images of molecules adsorbed on a surface are obtained while the tunneling tip is immersed in solution.[27] To obtain these images the molecule of interest is dissolved in a suitable nonpolar solvent. The solvent must be nonpolar to allow the tunneling current to be measured while the tip is under solution. In polar solvents the ionic current set up by the flow of dissolved ions can be large enough to prevent detection of the tunneling current (so far the tips used in these studies have typically not been coated with an insulating material as is normal for tips used in electrochemical STM). In addition, the solvent must have a low enough vapor pressure so that it does not evaporate during acquisition of images. The solvent selected must also be less strongly bound to the surface than the adsorbate of interest so that the adsorbate will not be displaced from the surface by the solvent. The typical physisorbed molecule is highly insulating with bandgaps (the energy difference between the highest occupied molecular orbital (HOMO) and the lowest unoccupied molecular orbital (LUMO)) on the order of 8−12 eV. Therefore, the adsorbate film must also be thin enough to allow for the tunneling electrons to flow between the tip and the substrate. As the diameter of the adsorbed molecules gets larger, a loss in resolution is observed (for example, STM images of DNA do not reveal the level of molecular detail seen with 8CB where different functional groups within the molecule can be resolved). Typical tunneling parameters used to image adsorbates are such that the gap resistance is on the order of 10^9−10^{10} Ω, so that the images are dominated by features of the adsorbed molecules and not the substrate.[27] This also helps prevent the tip from disturbing the molecules physisorbed at the liquid−solid interface.

For the STM to obtain high-resolution molecular images, molecules must be immobilized during the time that the tip scans over the surface. The systems that will be discussed here form highly ordered structures on graphite and appear to order as a two-dimensional crystal on the substrate. These molecules are typically large enough for thermal motion within the film to be slow at room temperature, allowing the adsorbate molecules to remain on the surface long enough to be imaged. The energetics favor molecules "plating out" at the liquid−solid interface; yet considerable evidence of dynamic motion can be observed, suggesting that the molecules move more or less freely, though slowly, between the surface and solution. As will be discussed below, the presence of solvent has a significant effect on the adsorption/desorption dynamics.

II.B. Studies of Hydrocarbons Physisorbed on Graphite. *Alkanes.* Thermodynamic studies of hydrocarbons adsorbed on the basal plane of graphite indicated that the heat of adsorption was large.[28−30] This was explained by the fortuitous match of the distance between the centers of the hexagons of the graphite lattice, 2.46 Å, and the distance between alternate methylene groups of the hydrocarbon backbone, 2.51 Å. This match allows the methylene groups to be located over the centers of the hexagons of the graphite lattice, providing approximately commensurate packing of the alkane molecules on graphite as schematically shown in Figure 1. This model[28−30] suggests that the molecular axes of the adsorbates are parallel to the graphite surface and that the molecular plane (containing the carbon atoms of the hydrocarbon backbone) is also parallel to the graphite substrate. This has been confirmed in a number of STM studies.[31]

The first STM images of alkanes adsorbed onto graphite from a solution were of the *n*-alkane, triacontane ($C_{30}H_{66}$, see Figure 2).[32] The STM images of dotriacontane reveal a highly ordered two-dimensional layer on graphite. The molecules lie in rows with adjacent rows parallel to each other, separated by narrow troughs. The width of each row was determined to be about 4.5 nm, which agrees well with the length of a dotriacontane molecule in its three-dimensional crystal structure (4.3 nm). This indicates that the molecules are lying with their molecular axes parallel to the graphite substrate. The alkyl chains appear to adopt an all-trans orientation on the surface, as indicated by their measured length, and the molecules are oriented at 90° with respect to the row direction. This is the same orientation exhibited by alkane molecules in their crystal structure.[33] The STM images correspond to a two-dimensional cut of the three-dimensional crystal structure. Following the observation of these images of dotriacontane other homologous *n*-alkanes ranging from nonadecane ($C_{19}H_{40}$) to pentacone ($C_{50}H_{102}$)[34−37] have been imaged. All these images were obtained under a liquid drop though with different solvents (for example, *n*-decane, phenyloctane, and

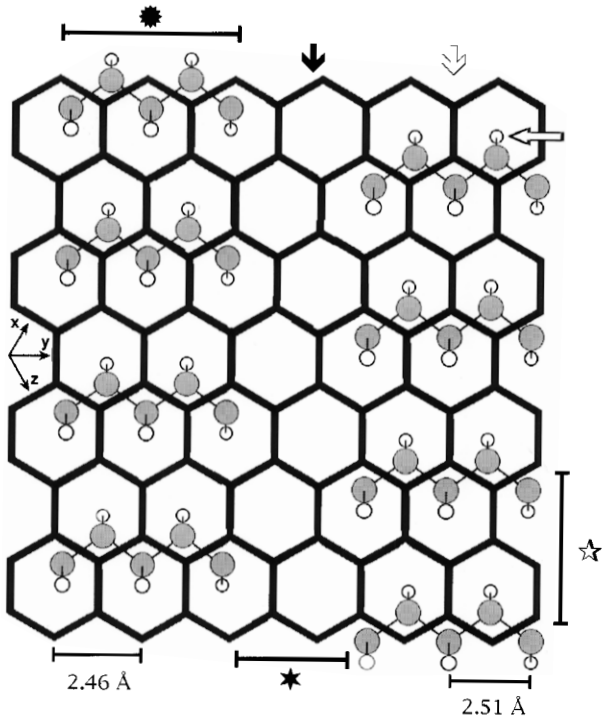

Figure 1. Schematic diagram of *n*-alkanes (C = ●, H = ○) adsorbed on a hexagonal graphite substrate. The alkanes lie in an all trans geometry with the molecular axis parallel to the graphite surface. The length of a molecule is shown by a bar marked by ∗. The molecules are observed to lie with their molecular axes parallel to the graphite lattice directions (*x*, *y*, *z*). The methylene hydrogens lie in the hollow sites of the graphite surface as indicated by ⟸. The molecules also self-assemble into ordered rows. The row direction and row width corresponding to one molecular length are marked by hollow down arrow and ∗, respectively. The spacing between molecules in a row is shown as a bar marked by ☆. A gap or trough (↓) separates the rows of molecules and the width is marked by a bar labeled with ★.

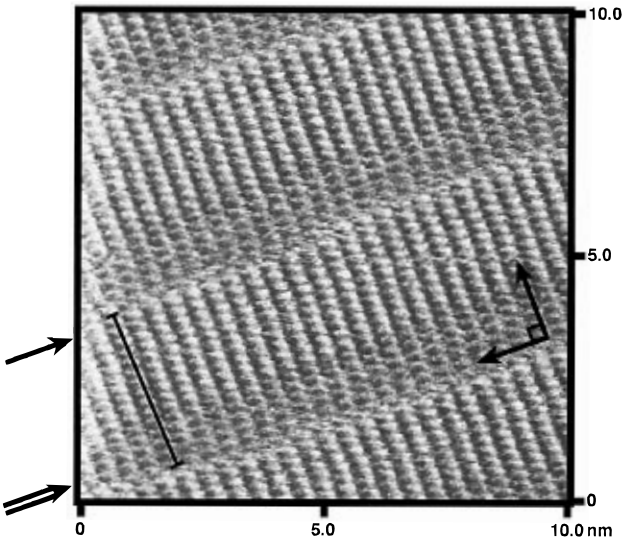

Figure 2. STM image of ordered rows of triacontane ($CH_3(CH_2)_{28}CH_3$) in phenyloctane on graphite. One molecular length is shown by a black bar. Fifteen spots are observed along the alkane backbone corresponding to one spot for every other methylene group in the alkyl chain. The mismatch of the carbon−carbon distance in the alkyl chain and the underlying graphite lattice is evidenced by the change in the STM contrast along the molecular axis. The bright end of the molecule is indicated by → and the relatively "darker" end is indicated by ⟹. The molecules are oriented with a 90° angle between the molecular axis and the direction of the lamellae. The 10 nm^2 image was obtained with a 1235 mV bias (sample negative) and a 166 pA setpoint in constant height mode. The gap resistance is 7.44×10^9 Ω.

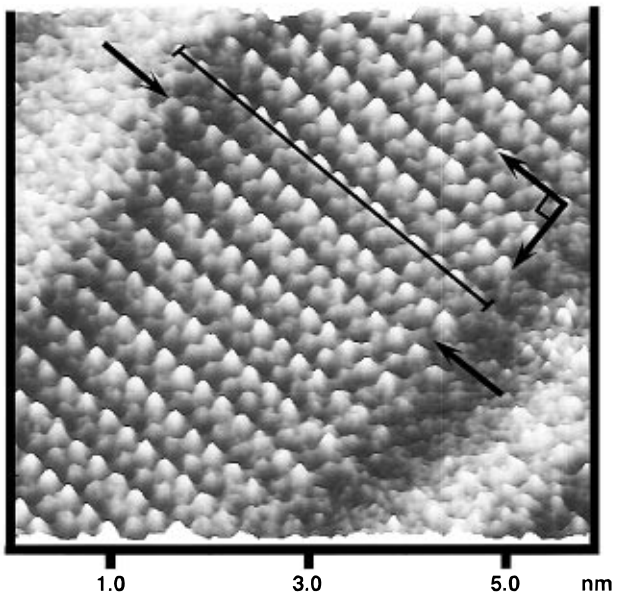

Figure 3. STM image of dotriacontane ($CH_3(CH_2)_{30}CH_3$) in phenyloctane on graphite. Each molecule consists of a double row of spots (indicated by the two arrows in the figure). One molecular length is shown by a black bar. Tunneling conditions used were −1400 mV (sample negative) and 194 pA in constant height mode (the image has been filtered with a lowpass filter). The gap resistance is 7.22×10^9 Ω.

diphenyl sulfide). The results obtained for these alkanes of varying length are similar to those for the dotriacontane showing highly ordered rows of molecules lying parallel to the substrate.

Close inspection of STM images of alkanes on graphite (in Figure 2) reveals a varying contrast along the length of an individual molecule, brighter at one end and dimmer at the other. This has been explained by the close but not perfect match of the distance between the hollows of the graphite lattice and the distance between alternate methylene groups. This slight mismatch creates an interference effect between the carbon chains of the molecules and the underlying substrate resulting in an intensity modulation along the length of the molecules.[34] Along the row direction, however, the molecules appear to be commensurate with the underlying graphite substrate.

High-resolution images of individual molecules reveal further structural detail along the lengths of the molecules. The number of "bumps" or "spots" along each molecule was typically found to be approximately half the number of carbon atoms in the molecules[36] and separated by ∼0.25 nm as shown in Figure 2. One study suggests that these spots correspond to those graphite lattice sites that are perturbed by the adsorbed molecules and hence "highlighted" in the STM images.[32] Another suggests that the observation of only half the methylene groups indicates that the molecular planes of these molecules lie perpendicular to the substrate, and hence the number of spots correspond to half the number of carbon atoms in the molecules.[34] More recent work reveals images where a double row of spots for every molecule is visible (see Figure 3).[38,39] The number of spots is approximately equal to the number of carbon atoms in the molecule, consistent with the molecules lying parallel to the surface. However, the distance and angles between spots in a double row do not agree with

the known distances and angles between carbon atoms in the hydrocarbon backbone, and hence the spots cannot be attributed to the carbon atoms in the molecules. The observed spacings are more consistent with the positions of the methylene hydrogen atoms. There is still debate regarding the orientation of the molecular plane (the plane containing the carbon atoms) with respect to the substrate. Orientations have been proposed from the STM images of *n*-alkane films in which the molecular plane lies parallel to the substrate,[32] perpendicular to the substrate,[34] flips back and forth between these two orientations[38] or has approximately a 30° angle between the molecular plane and the substrate.[39] The dynamics of the molecules within the physisorbed films may allow distinct orientations of molecules to be imaged at different times.

Large-scale images of alkanes on graphite show that these molecules remain ordered over the range that is scanned by the STM (hundreds of nanometers). In addition, domains are often observed where molecules in a given domain are oriented at 60° with respect to neighboring domains, consistent with the notion that the molecules follow the lattice directions of the hexagonal graphite substrate. Within each domain, the order and orientation of molecules is as described above. Domain boundaries are often regions of high mobility as indicated by the lack of resolution attained in imaging molecular orientation at the boundaries. Instability of domain boundaries is not always observed and seems to depend on the orientation of molecules at the boundaries. These domains do exhibit dynamics where one domain may grow at the expense of another.[34,35]

Alcohols. The high order exhibited by the alkanes adsorbed onto graphite is also observed for other hydrocarbons with the same methylene backbone but terminated with different functional groups. Terminally substituted monoalcohols (decanol ($C_{10}H_{21}OH$),[36] octadecanol ($C_{18}H_{37}OH$),[34] tetracosanol ($C_{24}H_{49}OH$),[34] docosanol ($C_{22}H_{45}OH$),[34] and triacontanol ($C_{30}H_{61}OH$)[34,35]) as well as alkyl chains terminated at both ends with an OH group (1,12-dodecanediol ($HOC_{12}H_{24}OH$)[34]) adsorbed on graphite have been imaged with the STM at the liquid−solid interface. The alcohol STM images also reveal a highly ordered layer of molecules as shown in Figure 4.

The presence of the OH group results in quite a different molecular orientation of the molecules within a row as well as the orientation of rows with respect to each other when compared with alkanes adsorbed on graphite. The molecules within a row are oriented with their molecular axes at an angle of 60° with respect to the row direction (see Figure 4), quite different from the 90° orientation exhibited by the alkanes. This orientation is also observed in the three-dimensional crystal structure of solid alcohols and has been attributed to hydrogen bonding between the OH groups of molecules in adjacent rows.[33] In some STM images indirect evidence of this hydrogen bonded network is visible, particularly for shorter alkyl chains, where the widths of the troughs between adjacent rows alternates between narrow and broad. The narrower trough arises from the closer packing of molecules brought about by hydrogen bonding between adjacent OH groups while the broader troughs mark the methyl ends of the molecules.

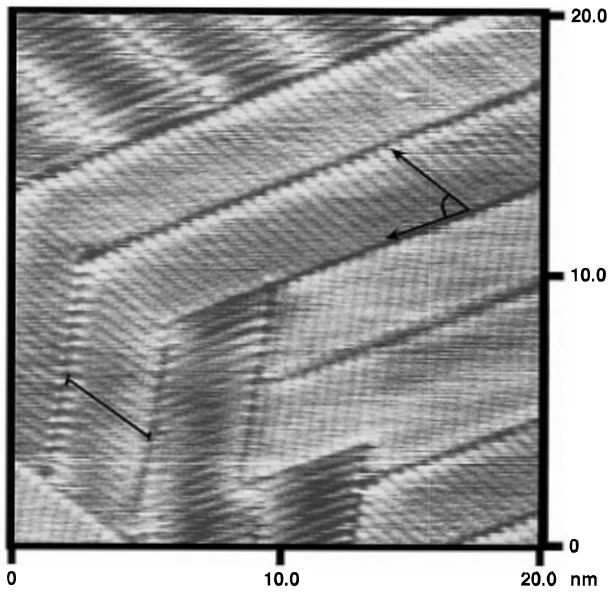

Figure 4. STM image of triacontanol ($CH_3(CH_2)_{29}OH$) in phenyloctane on graphite. One molecular length is indicated by a black bar. The molecules are oriented with a 60° angle between the molecular axis and the direction of the lamellae as indicated on the image. The 20 nm^2 image was obtained with a 1400 mV bias (sample negative) and an 80.0 pA setpoint in constant current mode. The gap resistance is 1.75×10^{10} Ω.

The alcohol rows also exhibit different behavior when compared with alkane rows. For alkanes, the rows run straight, often over hundreds of nanometers. Alcohol rows form zigzag patterns, changing direction by 120° typically every few nanometers.[34,35] The 60° orientation of the molecules within rows and the 3-fold symmetry of the underlying graphite allow for the change in direction resulting in these zigzag patterns.[34,35] The hydrogen-bonding network is maintained even for the molecules at the point where the rows change direction.[35] Hence, the system does not loose any energy by these changes in row direction. The change in direction of the alcohol rows appears to occur randomly, unrelated to defect surface sites.[34,35] In addition, these rows exhibit dynamical motion where the direction of the rows changes as a function of time. These molecular motions have been captured by a high scan speed STM, which sets the time scale for this process in the range of 10 ms.[34] As with the alkanes, the orientation of the alcohol molecular plane (parallel[32] or perpendicular[34] to the graphite substrate) is unresolved. While the presence of the OH groups in the alcohol molecules effects the molecular orientation and packing order of the molecules when compared with the alkanes, there is no direct visible evidence in the STM images as to the location of the OH group. At present the only reliable way to differentiate between images of alcohols and alkanes is to look at the molecular packing arrangement of an aggregate of molecules.

Carboxylic Acids. STM images of triacontanoic acid ($C_{29}H_{49}COOH$), stearic acid ($C_{17}H_{39}COOH$),[34,40] arachidic acid ($C_{19}H_{39}COOH$),[34,40] behenic acid ($C_{21}H_{43}COOH$),[40] and tetracosanoic acid ($C_{23}H_{47}COOH$)[34] adsorbed on graphite are all similar. These images reveal highly ordered two-dimensional layers with the molecules lying parallel to the substrate as shown in Figure 5. The acid molecules are arranged in rows with a 90° angle between the molecular axes and the row direction. For the acid molecules a 90° orientation permits hydrogen

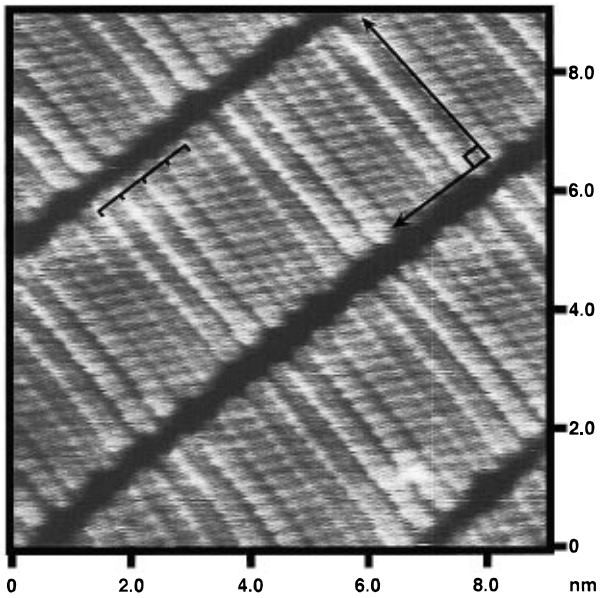

Figure 5. STM image of a carboxylic acid in phenyloctane on graphite. The molecules form a 90° angle to the direction of the row. A comb marks the 5 molecule repeat of the moiré pattern observed in the image. The 9.0 nm^2 image was obtained with a 1400 mV (sample negative) and a 230 pA setpoint in constant current mode. The gap resistance is 6.09×10^9 Ω.

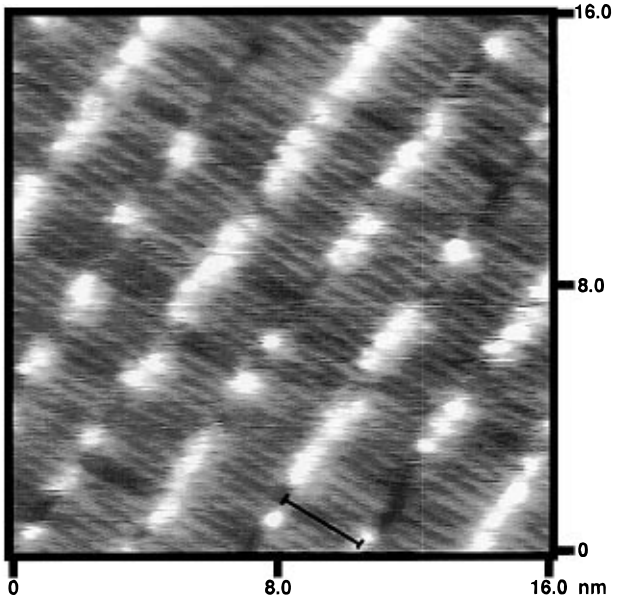

Figure 6. STM image of 1-docosanethiol ($CH_3(CH_2)_{21}SH$) in phenyloctane adsorbed on graphite. One molecular length is marked by a black bar. The bright spots dispersed over the image are attributed to the SH functional groups, and the bands at lower contrast connected to each bright spot are the alkyl chains. The angle between the molecular axis and the troughs between two rows is 90°. The 20 nm^2 image was obtained with a 1550 mV bias (sample negative) and a 150.0 pA setpoint in constant current mode. The gap resistance is 1.03×10^{10} Ω.

bonding between the carboxylic functional groups of the molecules in adjacent rows.

Close inspection of the STM images of long-chain carboxylic acids reveals an intensity modulation of the contrast in a direction perpendicular to the molecular axes, i.e., parallel to the row direction.[34,40] The periodicity of this modulation is about four or five molecular widths. This intensity modulation or Moiré pattern is not visible in images of alkanes and alcohols (compare Figures 2, 4, and 5, respectively). It has been suggested that the bulkier headgroups of the acids require more space as the molecules lie on the graphite.[34] As a result, the molecules are incommensurate with the graphite substrate along the row direction, resulting in an interference pattern between the adsorbed molecules and the substrate.[34] As with the alcohols, the position of the carboxylic head groups in the molecules cannot be unambiguously determined from the STM images.

Thiols, Sulfides, and Disulfides. Long-chain alkylthiols were imaged to determine how substitution of an S atom for an O atom effects packing and orientation of the molecules and the tunneling current when a smaller atom O ($r_{covalent}$ = 0.74 Å[41]) is replaced by a larger atom S ($r_{covalent}$ = 1.04 Å[41]).[42] An STM image of docosane thiol ($C_{22}H_{45}SH$) on graphite is shown in Figure 6. The most striking feature of this topograph is the presence of bright spots dispersed over the image. Visible at lower contrast are bands connected to these bright spots. The length of these bands agrees well with the length of a C_{22} carbon chain indicating that these bands correspond to the C_{22} alkyl chains. This suggests that the alkyl chains are oriented parallel to the graphite surface, which differs from the orientation of the alkylthiols on a gold surface. In the case of alkylthiols on gold, the molecules are chemisorbed on the gold surface through a S−Au bond causing the alkyl chains to orient at an angle to the gold surface.[43,44] The parallel orientation of the alkylthiols on graphite suggests that they are physisorbed on the graphite surface similar to other long-chain hydrocarbons.

From images similar to Figure 6, the alkylthiol molecules in a row appear to be oriented such that not all the SH groups lie on the same line.[42] In other words, the SH group of a molecule in one row does not necessarily face the SH group of a molecule in the adjacent row. This is quite different from the packing of the alcohols on graphite where all the OH groups of molecules in one row lie on the same line, and the OH groups of molecules in adjacent rows face one other so as to maximize hydrogen bonding. The fact that the alkylthiols are not all aligned with neighboring SH groups facing each other indicates that the relatively weak hydrogen bonding between the SH groups may not dominate the stabilization of these molecules on the surface as much as the hydrogen bonding in the alcohol films. This would also explain the difference in molecular orientation of the alcohols (molecular axes at 60° with respect to the rows) and the thiols (molecular axes at 90° with respect to the rows).

The STM clearly distinguishes the S atom from the C atoms in the alkyl chains, and the position of the S−H functional group in a molecule can be unambiguously located, which is not possible for the OH functional group in alcohols or the COOH functional group in carboxylic acids. Enhanced conductance in the vicinity of the sulfur groups has been observed in the STM images of other sulfur containing hydrocarbons including: docosane disulfide ($CH_3(CH_2)_{21}SS(CH_2)_{21}CH_3$),[42,45] octadecyl sulfide ($CH_3(CH_2)_{17}S(CH_2)_{17}CH_3$),[45] and dihexadecyl disulfide ($CH_3(CH_2)_{15}SS(CH_2)_{15}CH_3$).[31] This suggests that divalent sulfur is generally bright in these physisorbed thin films on graphite and MoS_2. While the mechanism leading to bright S atoms is not yet completely understood, being able to identify the position of an S atom in a molecule suggests that it may be

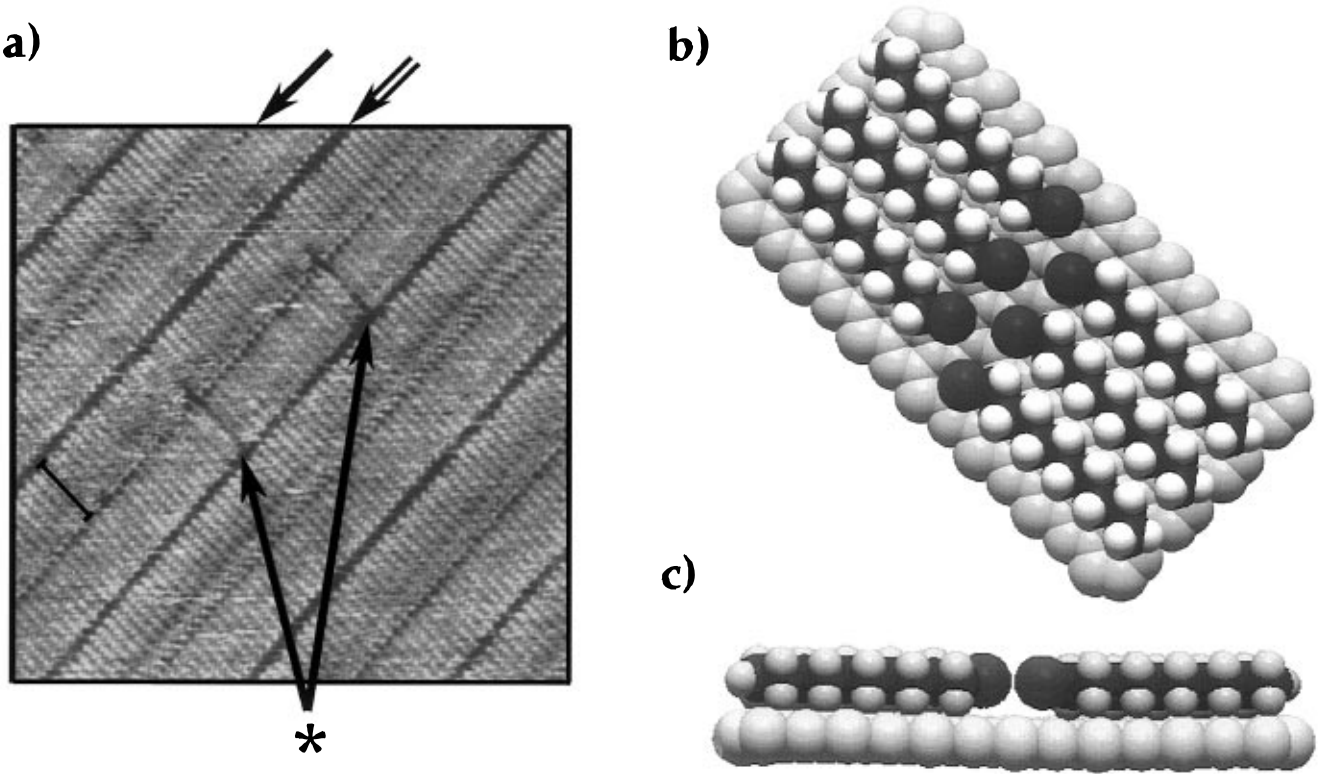

Figure 7. (a) STM image of 1-bromodocosane ($CH_3(CH_2)_{21}Br$) in phenyloctane on graphite. One molecular length is marked by a black bar. The troughs separating the rows of molecules indicated by → and ⇒, respectively, are not equivalent. The film has two defects, marked by an asterisk, which are also apparent in Figure 8. The 20 nm^2 image was obtained with a 1500 mV bias (sample negative) and a 400.0 pA setpoint in constant current mode. The gap resistance is 3.75×10^9 Ω. (b) Top view of a computer-generated model of a bromide film on a graphite substrate. In this model of the bromide film, the rows of molecules are paired with the bromides oriented "head to head". (c) Side view of the model in b shows that the bromine end groups lie in the plane of the film for an all trans conformation of the molecule.

possible to use S atoms as "markers" in molecules imaged by the STM.

Alkyl Halides. Unlike the images of the alkylthiols and alkyl disulfides, the images of chlorooctadecane on graphite[42] indicate that the contrast of the Cl-terminated ends and the rest of the molecule are the same. As with the alkanes, the angle between the molecular axis and a line drawn along the troughs between two rows is 90°. Films of docosane bromide on graphite, also display a 90° angle between the molecular axis and the direction of the lamella as shown in Figure 7. However, there is an alternating "wide" and "narrow" spacing between the rows. This alternating spacing suggests that the molecules in the rows are paired with the bromine ends lying head to head. In some cases, similar contrast is observed over the entire molecule and the bromine-terminated ends could not be differentiated from the methyl-terminated ends.[46] However, a reversible contrast change occurs in which the ends of the molecules in the "narrow" troughs are highlighted by a line of bright spots[46] as shown in Figure 8 (the nature of the contrast change is discussed below). In films of octadecyl iodides physisorbed on graphite, one end of the molecule is always observed as a bright spot, indicating that STM can also distinguish between the iodide functionality and the remainder of the alkyl chain.[46] Images of fluorine-substituted stearic acid films on graphite have also been imaged recently.[47] In these fluorinated stearic acid films both the carboxylic acid groups and the positions of the fluorine atoms are observed as dark spots in the STM image relative to the alkyl chain. It appears that while the STM is not able to differentiate between Cl and the alkyl chain, the locations of F, Br, and I substituents can be determined through variations in the STM contrast associated with each group relative to that of the alkyl chain. The nature of the contrast mechanism will be discussed below.

Cycloalkanes. In the solid crystalline state, cycloalkanes ($(CH_2)_n$) have the shape of a long rectangle with two long all-trans chains connected by two shorter chains of four CH_2 units.[48−50] The STM images of $(CH_2)_{48}$ and $(CH_2)_{72}$ adsorbed on graphite from a solution of the cycloalkane in dodecane reveal features very similar to those exhibited in the three-dimensional solid crystal structure[48−50] as shown in Figure 9. The images show a highly ordered layer of adsorbed molecules arranged in rows. The width of a row corresponds to the length of the long chains indicating that the molecules are arranged with the long chains perpendicular to a row direction. Bright and dim STM spots have been observed and attributed to the position of hydrogen atoms protruding out from each methylene group in the molecule; the bright spots corresponding to the hydrogen atoms of the most protruding methylene groups and the dimmer spots the positions of the hydrogen atoms along the long chains.[48−50]

Defects are visible in the ordered layer of the adsorbed cycloalkanes.[48] For example, in an adsorbed layer of $(CH_2)_{48}$, within a row are observed regions where four molecules are rotated at 90° with respect to the other molecules in the row. The combined width of four $(CH_2)_{48}$ molecules adds up to the length of one $(CH_2)_{48}$ molecule. Hence, this array of four molecules fits within a row and is easily incorporated without disturbing the overall 2-D structure of the interface.

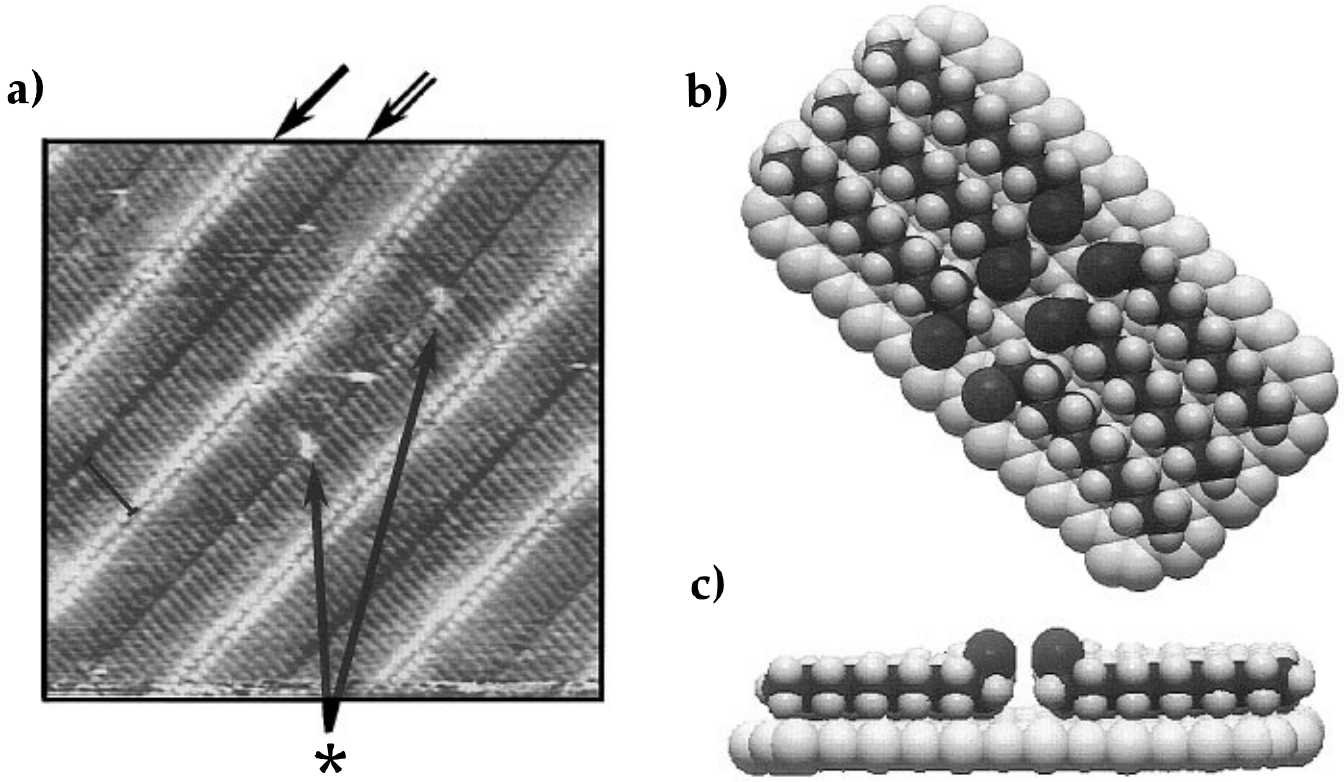

Figure 8. (a) STM image of 1-bromodocosane ($CH_3(CH_2)_{21}Br$) in phenyloctane on graphite taken approximately 10 min after the image in Figure 7a. No changes were made in the scan parameters between these images. The location of the bromines in the film are now indicated by bright spots at the ends of the molecule (→) and verify that the bromines lie "head to head". The film has two defects marked by an asterisk which are attributed to molecules with orientations opposite to the rest of the molecules in the film. These defects are also apparent in Figure 7a. The 20 nm^2 image was obtained with a 1500 mV bias (sample negative) and a 400.0 pA setpoint in constant current mode. The gap resistance is 3.75×10^9 Ω. (b) Top view of a computer-generated model of a bromide film on a graphite substrate. The bromide molecules shown in this model are in an end-gauche conformation in contrast to the all trans conformation shown in Figure 7b. The bromide molecules in this model were oriented in an end-gauche geometry *prior* to energy minimization in order to locate the local minima around this conformation. Rotation about the terminal RCH_2-CH_2Br bond from a trans to a gauche conformation may be responsible for the changes observed in the image contrast. (c) Side view of the model in b shows that the bromine points up out of the film when in the end gauche conformation.

Unsaturated Hydrocarbons. STM images of 10,12-octadecadiynoic acid[31] and *trans*-9-octadecenoic acid[40] show ordered two-dimensional crystalline layers on graphite. For the octadecadiynoic acid[31] the alkyl chains are perpendicular to the row directions and the carbon backbone is parallel with the substrate. The diacetylene groups are tilted at an angle of 45° with respect to the alkyl chains. Images of both molecules indicate higher tunneling currents over the C≡C triple bonds compared with the alkyl chains.

Mixtures of Hydrocarbons. Some of the first images of mixtures of different chain length alcohols adsorbed on graphite were due to impurities of higher chain homologues in a sample of alcohols.[34,35] These images indicate that the longer chain lengths prefer to lie next to each other so as to have optimum overlap along the entire length of each molecule. However, while the longer chains do segregate on the surface, there are no empty spaces around these longer chains. In fact, the shorter chains arrange themselves around these longer impurity molecules in such a way as to optimize intermolecular interactions between neighboring chains.

Mixtures of carboxylic acids of different lengths have been imaged at the solid−liquid interface.[37] These images show that the mixture phase separates on the surface to form segregated domains of molecules with the same chain lengths. In equal proportions, molecules with the longer chain length have a higher surface coverage. This agrees with thermodynamic studies which indicate that the heat of adsorption of hydrocarbons on graphite increases with chain length.[28−30]

A study of a mixture of a straight-chain alkane and a cycloalkane indicates that the cycloalkane can displace the straight-chain alkane from a graphite surface.[49] A particularly intriguing feature of this study is the suggestion that in some regions of the surface, the cycloalkane forms the first adsorbed layer on graphite and the linear alkane forms an epitaxial layer on top of the cycloalkane layer. Such STM images of bilayers have been reported in other studies of hydrocarbons.[37,45,50]

The different molecular orientations of alcohols and alkanes adsorbed on graphite were used to study a mixture of triacontane ($C_{30}H_{62}$) and triacontanol ($C_{30}H_{61}OH$) adsorbed onto graphite from a phenyloctane solution.[35] The images of the alcohol/alkane mixtures show that separation into an alcohol and an alkane phase occurs on the surface. For 1:1 mixtures of triacontane/triacontanol in phenyloctane the ratio of the surface coverage of the alcohols to that of the alkanes on the surface was determined to be about 7:3.

This preferential deposition of the triacontanol molecules is due to a difference in the difference of free energy between solution and surface adsorbed molecules for the alcohols and alkanes of only 0.5 kcal/mol ($\Delta(\Delta G)/RT = \ln(^7/_3)$). This small difference accounts for the fact that alcohol molecules are observed on the surface about twice as often as alkane molecules. The stabilization

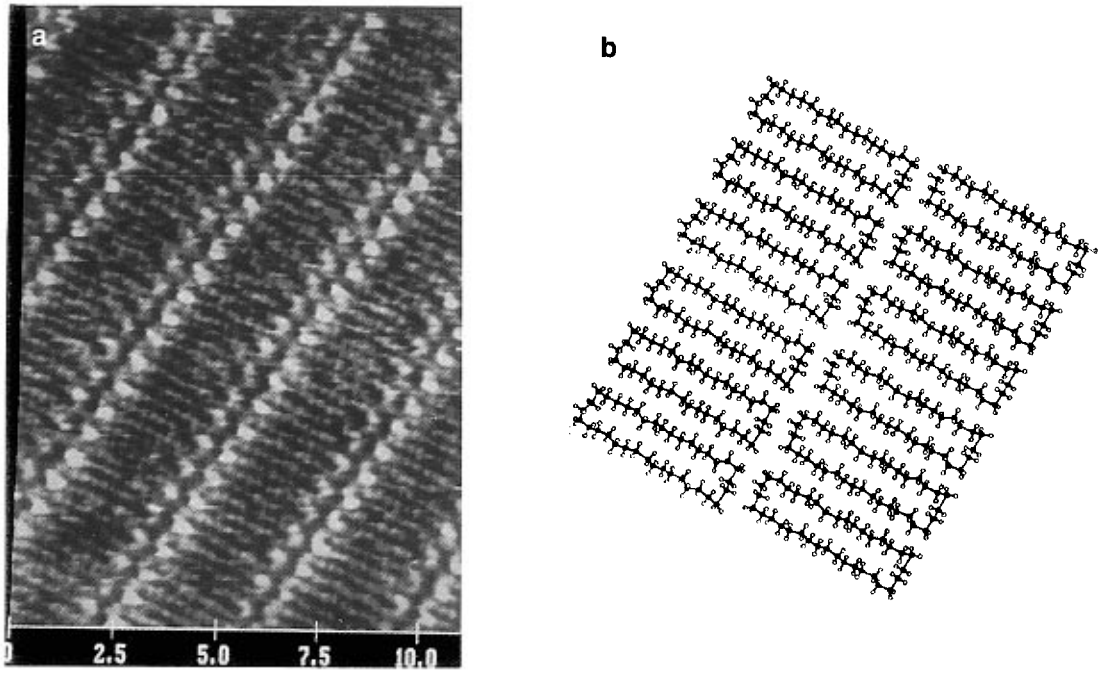

Figure 9. (a) STM image of a cycloalkane film $(CH_2)_{48}$ on graphite registered at 1100 mV bias (sample negative) and a 300 pA setpoint in constant current mode. The gap resistance is 3.66×10^9 Ω. The scales in the image are in nm. Reproduced from ref 50 with permission from Prof. M.-H. Whangbo and Dr. S. N. Magonov. (b) Schematic representation of the lamella arrangement of $(CH_2)_{36}$ molecules in the (101) crystallographic plane. Reproduced from ref 50 with permission from Prof. M.-H. Whangbo and Dr. S. N. Magonov.

gained by hydrogen bonding and the solvation energy are expected to play a role in the differential adsorption process.

Aromatic Derivatives. STM images of liquid crystals with aromatic rings and aliphatic side chains indicate that the tunneling current over the aromatic cores is larger than that over the aliphatic chains.[5−9,26] The aromatic rings appear as bright features in the images, and the aliphatic chains are visible with lower contrast. The mechanism via which the tunneling current is enhanced over the aromatic cores is still not clearly understood (see below). Since the initial studies of liquid crystals, other molecules with aromatic cores have been imaged, and all show an enhanced tunneling current over these aromatic rings. Systems that have been imaged at the solid−liquid interface include 1,4-didodecylbenzene,[31,34] 1,5-didecloxynaphthalene,[31] hexakis(heptyldecyloxy)triphenylene,[31,51] hexakis(hexadecyloxy)triphenylene,[31,51] and a series of mixed thiophene−*N*-alkylpyrrole oligomeric molecules.[52] All of these molecules form ordered two-dimensional layers on graphite.

Typical of these are hexakis(alkoxy)triphenylene derivatives, which exhibit a discotic liquid-crystalline phase. STM was used to determine the packing order and investigate the dynamics of the formation of the first ordered layer of these molecules adsorbed on graphite, as well as how molecules such as these, which posses a 3-fold symmetry axis, order in two dimensions.[31,51] The systems investigated were hexakis(heptyloxy)triphenylene (T_7) and hexakis(hexadecyloxy)triphenylene (T_{16}), where the two differ by the length of the alkyl chain attached to the alkoxy group.[31,51]

The STM images of both T_7 and T_{16} clearly show the position of the triphenylene cores as bright features. As observed in molecules with aromatic rings,[5−9,26] the tunneling current over the triphenylene groups is larger than that over the alkyl chains. Both molecules exhibit ordered two-dimensional layers, but the orientation of the triphenylene cores are different. For the T_7 molecules, the orientation of the triphenylenes alternate from row to row. The alkyl chains could not be resolved presumably due to motion of these side chains. In general, the shorter the carbon chain length the larger the thermal motion making the chains harder to image. The T_{16} molecules however are oriented with the triphenylene groups all in the same direction. Here the longer C chains are visible in the images, though at a lower contrast than the aromatic rings. Orientation of the triphenylene groups in the same direction stabilize the layer by allowing the alkyl side chains to be parallel with one another.

II.C. Adsorbates on Other Substrates. Most STM studies of molecules adsorbed at the liquid−solid interface have used graphite as the supporting substrate. The hydrocarbon systems described above seem particularly well suited for adsorption on graphite due to the close match between molecular and lattice parameters (see Figure 2). The result appears to be the formation of highly ordered two-dimensional layers for these molecules on graphite. However, other substrates can be used as supports for ordered layers.

Studies of liquid crystals on molybdenum sulfide (MoS_2) indicate that on this substrate ordered layers do form.[10,11,26] However, the packing order of the molecules adsorbed on MoS_2 can be quite different than that on a graphite substrate. For example, the liquid-crystal 8CB on graphite displays a head-to-head orientation within a row, whereas on MoS_2 the 8CB molecules alternate between a head-to-head and tail-to-tail orientation within the same row.[26] For 10CB and 12CB, however, the packing order on graphite and MoS_2 are similar.[26] The intermolecular spacings for these molecules are different on the two substrates presumably because of the different lattice constants (MoS_2, 3.16 Å; graphite, 2.46 Å).

STM images of dotriacontane ($C_{32}H_{66}$) on MoS_2 and $MoSe_2$ (lattice constant 3.29 Å) indicate that ordered layers can form on substrates even if there is a mismatch between molecular and lattice parameters.[53] For example, images of dotriacontane on $MoSe_2$ reveal ordered rows of molecules.[53] However, the substrate does seem to have quite a dramatic effect on the orientation of molecules within the rows. As opposed to alkane molecules lying with their molecular axes perpendicular to the row direction on graphite, on $MoSe_2$ the molecular axes lie at an angle of about 30° with respect to the row direction. In some areas on the surface, molecules exhibit a herringbone pattern alternating between a +30° and a −30° orientation, while in others all molecules in adjacent rows have the same orientation. At lower bias voltage where features of both adsorbate and substrate are visible, the molecular axes are found to be parallel with a lattice vector of the substrate (similar to graphite).

In general, these studies indicate that an atomically flat substrate is the most important surface property in forming an ordered layer.[53] The substrate surface need not have lattice constants that match with molecular parameters (as do graphite and long alkyl chains) for film formation. However, there is evidence that the orientation of molecules with respect to each other within the film is influenced by the surface's lattice constants and appears to be determined by an interplay between molecule−molecule interactions and molecule−surface interactions.

The fact that an atomically flat surface is the key factor required to form ordered layers is further strengthened by images of molecules adsorbed on β-Nb_3I_8.[50] The lattice constant for this surface is 7.60 Å, considerably larger than that of graphite. In this crystal, each layer has a Nb atom sandwiched between two iodine atom sheets. The crystal structure of β-Nb_3I_8 is such as to cause the surface to have "grooves" along three directions oriented at 60° with respect to one another. This "grooved" surface is, therefore, not atomically flat as are graphite, MoS_2, and $MoSe_2$. Attempts to image cycloalkanes on β-Nb_3I_8 were not successful.[50] Images of n-$C_{36}H_{74}$ on β-Nb_3I_8 display a very different packing order than do images of n-$C_{36}H_{74}$ on graphite.[50] STM topographs of this molecule show bright features separated by about 3.8 nm (as shown in Figure 10), and the images have been interpreted as a molecule lying in each groove with the end of the carbon chain protruding up out of the groove.

II.D. Scanning Force Microscopy (SFM) Studies of Physisorbed Molecular Films at the Liquid−Solid Interface. Comparison of SFM images and STM images of the same adsorbates should provide insight into the variations in contrast observed over different functional groups. For example, are the contrast variations due to electronic differences or topographic differences? SFM images are more sensitive in revealing topographic information on a surface while STM images are also sensitive to the electronic properties of the sample. Although SFM has been used to image chemisorbed species, imaging physisorbed adsorbates is more difficult. The weak interaction between the adsorbate and the substrate may be easily disturbed by the SFM tip resulting in damage to the adsorbed film. In addition, to obtain molecularly and atomically resolved images with the SFM is generally more difficult then

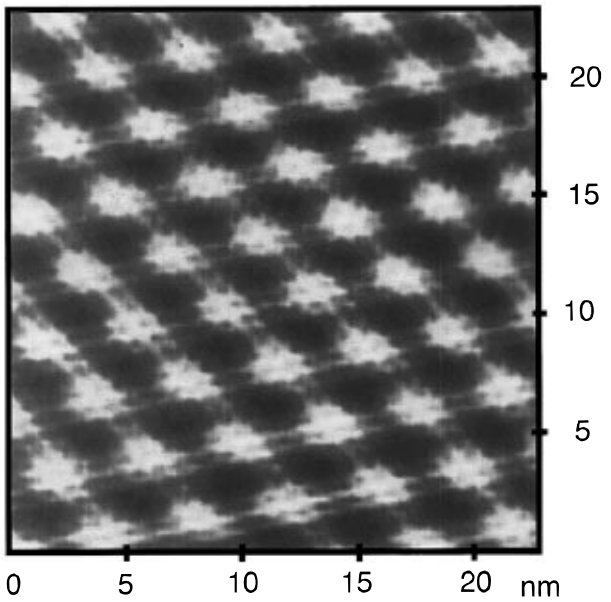

Figure 10. A 25 nm^2 STM image of $C_{36}H_{74}$ on β-Nb_3I_8 with a bias voltage of 485 mV (sample positive) and a 690 pA setpoint. The gap resistance is 7.03×10^8 Ω. Reproduced from ref 50 with permission from Prof. M.-H. Whangbo and Dr. S. N. Magonov.

with STM. Nevertheless, by using extremely small forces (less than 1×10^{-9} N) SFM images of octadecanol ($C_{18}H_{37}OH$) layers at the graphite solid−liquid interface have been obtained.[54] As long as the tip−sample interaction force was below about 1×10^{-9} N, images of ordered layers of alcohol molecules on graphite were obtained. Raising the force above this value resulted in images of graphite indicating that the tip had removed the alcohol monolayer. Molecularly resolved images were obtained and comparison with STM images of octadecanol revealed similar features (molecules arranged in rows, with the width of a row corresponding to the length of a molecule, etc.). In the SFM images, the troughs between two rows are not dark but instead revealed bright lines running parallel to the rows, which are attributed to topographic differences between the end groups and the methylene backbone. Similar contrast modulations are visible in the troughs of octadecanol molecules on graphite in STM images.[54] This similarity between the SFM and STM images suggests that the STM signal arises from a topographic difference between the OH ends and CH_3 ends and not necessarily a difference in electronic properties.[54]

A particularly pretty demonstration of the energy required to move dodecanol molecules out of the way of a scanning tip, as a function of distance from a graphite surface, has been provided by an AFM study of this liquid/surface system.[55] Molecular order induced in the liquid by the solid surface can change the short-range forces acting between two solids in a liquid medium. The force measured normal to the surface shows that the AFM tip encounters a series of repulsive walls as it approaches the surface at constant speed. The periodicity of the steps in the force are commensurate with the size of the dodecanol molecules and the magnitude of the repulsive steps varies from 5−1000 kT as a function of distance from the surface.

AFM studies also provide a particularly convenient method of studying surfactants at the liquid−solid interface, since the surfactant structures are large and

the solutions are charged making application of STM techniques slightly problematic. Direct images of quaternary ammonium surfactant aggregates have been obtained which are consistent with half-cylinder structures on crystalline hydrophobic surfaces, full cylinders on mica, and spheres on amorphous silica all in aqueous solution.[56] These structures appear to result from a compromise between the natural free curvature as defined by intermolecular interactions and the constraints imposed by specific surfactant−surface interactions.

III. Tunneling Mechanisms

The successful imaging of numerous physisorbed organic films at solution/solid interfaces (described above) has also demonstrated that the STM is sensitive enough to differentiate between different functionalities within these films. The origin of the image contrast in these organic films is a subject of debate, since organic molecules, with typical HOMO−LUMO gaps on the order of ∼8−12 eV, are insulators. The STM images of bare metal surfaces have been interpreted as measuring the total local density of states (LDOS) at the Fermi level of the sample surface at the position probed by the tip.[1] The tip−adsorbate−surface system can be considered a two-barrier problem with the additional possibility that discreet molecular states participate in the tunneling process. While the exact location of the molecular adsorbate electronic states with respect to the surface Fermi level is generally not known, a number of studies locate the conduction band for *n*-alkanes, Xe, and CH_3Br just below the vacuum level[57−62] and several electronvolts above the substrate Fermi level. Despite this fact, the STM images of molecular adsorbates often correlate well with the shape of the HOMO and LUMO of the molecule suggesting that the frontier orbitals of these species participate in the tunneling process.[15,31,63,64] A vigorous discussion concerning the relative participation of molecular states in the tunneling process has developed in recent years.[1,38,59,65−76]

III.A. Perturbation of the Local Surface Work Function. One initial hypothesis about the origin of the STM contrast for molecular adsorbates suggested that direct participation of the adsorbate levels was not necessary; rather, the contrast mechanism responsible for the near atomic resolution of molecular adsorbates was ascribed to a modulation of the local work function (tunnel barrier) of the substrate surface by the polarizable adsorbate.[77] Changes in the macroscopic work function of clean metals by adsorbates have been well characterized.[78] From this perspective adsorbates are imaged through perturbation of the "local" work function over the adsorbate, without direct participation of the electronic states of the molecule. For example, cyclohexane and benzene on graphite are observed with similar STM contrast and these molecules have very similar polarizabilities but very different electronic structures.

III.B. Resonant Tunneling. Other groups have proposed that molecular states may participate in the tunneling process directly when imaging liquid-crystalline 8CB films[79] and isolated DNA strands[80] on graphite. In both cases, it was suggested that at the bias voltages used for imaging these systems the molecular states may be accessed as intermediates in the tunneling process. In such a case the electrons tunneling from the tip to the sample are temporarily localized in molecular states that facilitate the tunneling process and increase the tunneling conductance in the vicinity of the adsorbate. These "quasibound states" allow resonant tunneling of the electron through the adsorbate and correspond to a resonance between the empty molecular states of the molecule and the surface electron levels. It has been suggested for films of 6CB on graphite that the cyanobiphenyl groups' π orbitals are close in energy to the π orbitals in the graphite surface.[50] Therefore, the π orbitals mix more strongly with the graphite surface than do the orbitals of the alkyl chains and consequently the cyanobiphenyl groups exhibit a much brighter contrast in the STM image than the alkyl groups.[50]

While the unperturbed states of DNA may lie far from the substrate's Fermi level, tip-induced pressure on the sample could shift the energy levels of the adsorbate closer to resonance with the Fermi level.[69−71] Pressures of ∼1 GPa are observed to shift the UV adsorption spectra of DNA as much as 0.5 eV.[69] A dipolar adsorbate state with an initial energy of 5 eV and a width of 0.5 eV, for example, may be shifted by 1 eV and broadened by 0.1 eV as a result of a 10 GPa pressure change induced by the STM tip.[69] This fairly substantial shift of 1 eV may be enough to bring an "outlying" adsorbate state into resonance with the Fermi level of the surface for participation in the tunneling process. Tip-induced, pressure-dependent STM contrast has also been suggested as a mechanism for contrast variation in the imaging of bilayers of *n*-$C_{36}H_{74}$ alkanes on graphite.[81]

III.C. Weak Electronic Coupling. Physisorbed Xe atoms on Ni are observed with an unexpectedly strong contrast as a protrusion of about 1.53 Å above a bare Ni surface.[59] The strong contrast and the large energy gap between the highest occupied atomic orbital and the lowest unoccupied atomic orbital of the isolated atomic Xe adsorbate (quite similar to the HOMO−LUMO gaps of the organic molecules of interest here) make this system an interesting prototype for understanding the nature of the STM contrast of physisorbed species in general. The relative contribution of energetic and spatial overlap between the tip and sample states in the Xe on Ni system were explored using an atom-on-jellium model.[59] The contribution of the Xe adsorbate's unoccupied 6s state (4 eV above the surface Fermi level) to the LDOS was calculated at a distance of ∼11 bohr from the surface (the region probed by the STM tip). This calculation revealed that the contribution of the Xe adsorbate to the LDOS of the Xe/Ni system is peaked 0.5 eV below the vacuum level, in agreement with experiment (see Figure 11). The contribution of the Xe to the local density of states at energies near the Ni Fermi level (far from the peak of the adsorbate resonance) is small and does not change very much with energy. Since the tunneling probability depends on the local density of states at the Fermi level, the imaging of adsorbates should not depend sensitively on the electronic structure of the adsorbate as long as the energy difference between the frontier orbitals and the Fermi level of the surface is large. On the other hand if the adsorbate level approaches within ∼0.5 eV of the surface Fermi level, this picture predicts that the tunneling current should be a strong function of the adsorbate's electronic structure.

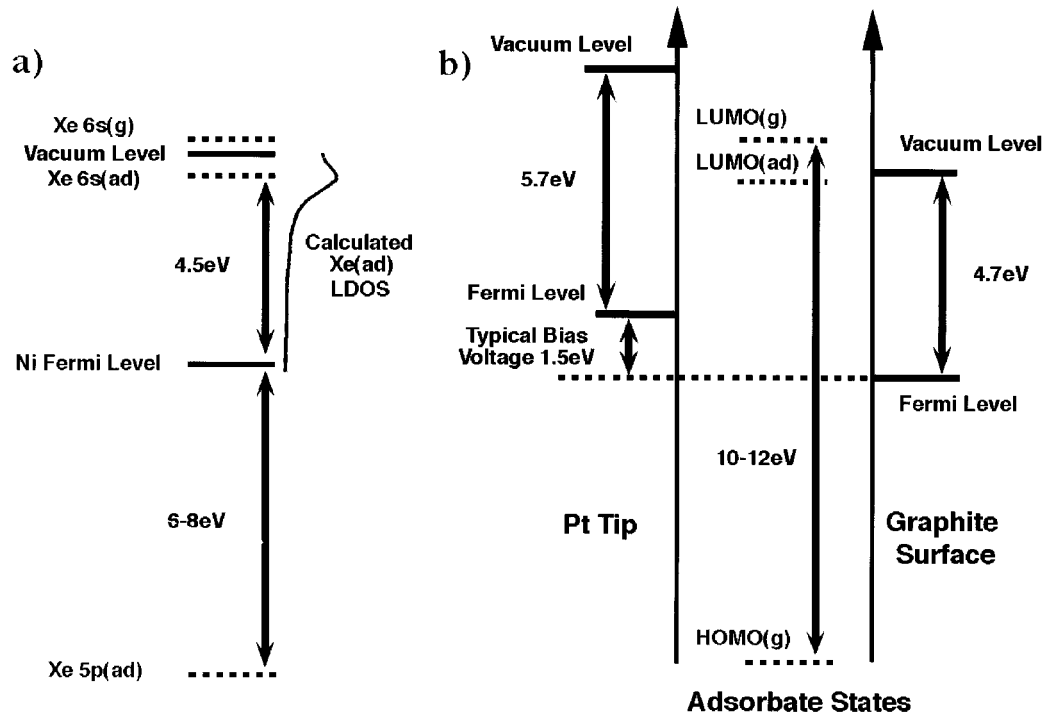

Figure 11. (a) Energy level diagram for Xe adsorbed on a Ni surface. Both the highest occupied Xe 5p and lowest unoccupied Xe 6s levels lie far in energy from the Ni Fermi level. Prior to adsorption, the gas phase Xe 6s(g) level lies just above the vacuum level. Upon adsorption the Xe 6s(ad) is lowered ~0.5 eV below the vacuum level by the heat of adsorption. Lang's atom on jellium calculation of the contribution of the Xe(ad) to the local density of states of the surface/adsorbate complex reveals that the resonance corresponding to the Xe 6s(ad) state is broadened upon adsorption and develops a long energy tail which extends to the Ni Fermi level.[59] (b) General qualitative energy level diagram for a molecular adsorbate on graphite with a typical HOMO−LUMO gap of 10−12 eV. Organic molecules are normally insulators and the location of the HOMO and LUMO in the tunnel junction is not well defined. However, by analogy with the Xe on Ni states in Figure 11a, the adsorbate levels most likely lie far in energy (several electronvolts) from the Fermi levels of the graphite substrate and the Pt tip.

Another key feature of the atom on jellium calculations for the Xe on Ni systems is that despite the weak mixing of the Xe 6s and the surface Fermi level electronic wave functions, the contribution of the adsorbate to the local density of states at the Fermi level is ~2 orders of magnitude larger than the contribution of the bare substrate to the LDOS at the large distances (roughly 11 bohr in the case of Xe on Ni) from the surface typically probed by the STM tip in an experiment where adsorbates are being imaged.[59] These observations suggest that Xe becomes visible in the STM because the Xe adsorbate spatially dominates the region probed by the STM tip, despite the Xe 6s(ad) level's weak mixing with the Fermi level surface wave function.

Xe physisorbed on Ni, with a 5p−6s gap of ~12 eV, appears to be the atomic analogue of the insulating molecular adsorbates described here since organic molecules typically have large HOMO−LUMO gaps of 8−12 eV. While the exact placement of the adsorbate levels with respect to the surface Fermi level is uncertain in the case of organic adsorbates, the frontier orbitals of the molecular adsorbates, like the Xe 6s on Ni, almost certainly lie several electronvolts away from the Fermi level of the graphite surface or the Pt tip. By analogy to Xe on Ni, the frontier orbitals of insulating organic molecules should participate in the tunneling process through a weak mixing of the adsorbate LUMO and the electronic levels of the graphite at the Fermi level. The spatial extension of the molecule away from the surface pushes the mixed adsorbate/surface electronic wave function out from the surface where the contribution of the bare graphite to the Fermi level LDOS is negligible. This may explain how the tunneling electrons can couple to the molecular framework of these insulating molecules and why the shapes observed with the STM sometimes resemble the shape of the frontier orbitals.

In another approach, the electron scattering quantum mechanical method has been used in order to explain the electronic origin of the submolecular internal features in the STM images of benzene on graphite and the relative participation of the molecular and substrate states to the STM image.[67,82,83] In this picture the tunneling mechanism can be viewed as arising from two types of electronic interactions: (1) "through space" (TS), which describes the direct coupling of the tip and the metal surface, and (2) "through molecule" (TM), which includes the coupling mediated by the electronic levels of the molecule in the tip−adsorbate−substrate system. In the TM electron-transport mechanism (similar to the atom-on-jellium model[59]) the coupling with the substrate states through the molecule originates from the "tails" of molecular electronic states closest to the Fermi level. The overall STM image is the interference between the TM and TS tunneling mechanisms. While the TS coupling is enhanced in the vicinity of the molecule, this is not the main origin of contrast under the conditions required for molecular imaging. The TM coupling displays much stronger corrugation and is responsible for the submolecular internal structure observed in the STM images.[82]

This approach has been remarkably productive in modeling the effect of substrate adsorption site and tip apex structure on the contrast of the STM images of atomic and aromatic adsorbates.[83] Tip structure variations are most noticeable as changes in the STM image resolution and can also cause contrast reversal. Mo-

lecular orbitals close to the Fermi level are found to contribute strongly to the image contrast, but states farther from the Fermi level will also contribute if they have good spatial overlap with the tip.

III.D. Voltage Dependence of the STM Image Contrast. There have been several reports that the STM image contrast of functionalized alkanes does not depend strongly on bias voltage.[9,40,46,79,80,84−86] Above a certain threshold bias voltage (>±0.5 eV) the STM image is dominated by molecular features. In many cases, little contrast change is observed as the bias voltage is varied over a broad range (±2.0−0.5 eV). Below this voltage, a very smooth transition between the molecular images recorded at higher voltages and lower setpoint currents (corresponding to large sample/tip distances), and images which reflect the substrate structure at lower voltages and high setpoint currents (corresponding to small sample/tip distances) are observed. The STM images also tend to be insensitive to the polarity of the bias voltage consistent with a picture where molecules are being imaged through an energetically diffuse state, or the tails of the molecular resonances in the tunnel gap.

III.E. Effects of Adsorbate Orientation on the STM Image Contrast. The relative contribution of TS and TM tunneling provides STM sensitivity to the orientation of a molecule *parallel* to the surface and is responsible for the appearance of moiré patterns when there is a lattice mismatch between the ordered adsorbate film and substrate periodicity. The interference between the contributions of the TS and TM electron tunneling mechanism, for example, has been used to explain the moiré patterns observed in STM images of carboxylic acid films physisorbed on graphite.

Recently, a general theoretical formalism which includes quantum interference effects, has been used to describe how the lateral and height (z) resolution of the STM can be employed to distinguish between flat and tilted molecular orientations with respect to the surface.[68] The results of this study are consistent with the proposal that the "spots" in the STM images of alkanes correspond to the locations of the hydrogen atoms along the alkyl chain rather than to the positions of the tetrahedrally bonded carbons in the alkyl backbone.[75] The methylene hydrogens are the outer most atoms on the molecule and, thereby, have the most effective overlap with the STM tip during scanning of the sample. Similarly, time-dependent variations observed in the STM image contrast in films of 5CB and 4CB on graphite have been attributed to tip induced changes in the "tilt" or orientation of adsorbates perpendicular to the surface.[80]

III.F. Examples of Topographic and Electronic Effects on Image Contrast. Effects of sample topography on the STM image contrast have been observed in the comparison of the relative "brightness" of a series of different functional groups with respect to the carbon chain in monolayer films of primary substituted hydrocarbons ($CH_3(CH_2)_nCH_2X$; X = CH_3, OH, Cl, NH_2, SH, Br, I; n = 16−30) adsorbed on graphite from a solution of phenyloctane.[46] Functional groups characterized by larger polarizabilities, a measure of physical size, display a stronger contrast in the STM. The NH_2, SH, Br, and I are all observed as bright spots at the end of the alkyl chain. Insensitivity to the bias voltage is observed for these molecules (0.5−2.0 eV) and has also been reported for tunneling spectroscopy of an alkyl cyanobiphenyl liquid-crystal film.[85]

The physical size of the functional group does not appear to be the only factor governing the tunneling current in these systems. The "bright" bromine end groups in the films of 1-bromodocosane on graphite undergo a reversible contrast change (from dark to bright, see Figures 7 and 8, respectively) with time, without loss of resolution along the alkyl chain. For the 1-bromodocosane films, rotational isomerization is energetically feasible at room temperature,[87−90] since the barrier to rotation of the bromine end group is small, and the energy difference between two rotamers (trans and gauche, see Figures 7b,c and 8b,c, respectively) is only ∼0.1 kcal/mol.[91,92] In the all-trans conformation the molecule may lie flat with the terminal C−Br bond parallel to the surface. Reorientation of the bromine end groups from the trans to the gauche conformation would push the Br up out of the plane of the film leading to a more favorable spatial overlap with the tip, thereby modulating the image contrast. Evidence of tumbling motions of alkanes about their long axis in the film have also been observed as changes in the alkyl hydrogens' positions relative to the surface.[38] In this regard, film dynamics, involving a cooperative rotation of the molecules in the film about their molecular axes or concerted reorientation of the end groups,[87−90] may be responsible for the contrast variations observed in the bromide films.

Fluorinated stearic acid films on graphite have been examined in an attempt to distinguish between electronic and topographic effects of molecular adsorbates on the STM contrast.[47] A reduced tunnel current marks the location of the F atom in the fluorinated stearic acid film. Since only small changes in the topography are expected upon F substitution, the reduced current which characterizes the location of the fluorine is attributed to the electronic structure of the fluorinated stearic acid film and emphasizes the difficulty of interpreting the STM images as simply a reflection of the topography of the sample.

IV. Dynamics

IV.A. Molecular Dynamics Simulations. There have been a number of simulations of the self-assembly of long-chain molecules at the liquid−solid interface.[93−98] Such investigations are very useful in providing a microscopic, molecular scale view of the dynamic processes that lead to the kinds of structures observed in STM studies of interfaces. For the most part the time scale for the rate-limiting processes that determine the structures and organization for molecules adsorbed on surfaces are far too short to be observed by present STM techniques. Hence, model molecular dynamics simulations provide useful clues to the physical and chemical driving forces that control molecular assembly.

Insight into the interplay between entropy and enthalpy in the assembly of long chain $C_{24}H_{50}$ on graphite was provided by a molecular dynamics study that did not include any solvent.[93] These simulations confirm the experimental observation that long-chain alkanes adsorb parallel to the surface of graphite. This study also suggests that molecular arrangements with the carbon zigzag plane perpendicular to the surface are more stable than those with the carbon plane parallel to the surface. The differences in conformation between

parallel and perpendicular orientations of the carbon zigzag plane are found to be driven by a subtle combination of entropy effects, which decrease the stability of the more densely packed, laterally confined parallel structures, and surface adsorption energy, which stabilizes these same structures. The relatively small differences in stabilization energy between the two structures is not sufficient to overcome the higher entropy disadvantage of having the zigzag structure parallel to the graphite surface. The time scale for molecules to reach their equilibrium geometry on the surface was found to be approximately 30 ps. A slight communal tilt of the molecules within a lamella is also observed and found to be sensitive to the packing density. Experimental evidence for concerted flipping between tilted and untilted structures was also presented, although this flipping must take place on a time scale long compared to that accessible to MD simulations. Studies of the structure of multiple layers of molecules can also be made using molecular dynamics simulations. Here, the separation of the film's first layer from the surface is found to be well localized in the normal direction, while successive layers lying further from the surface are found to be more and more smeared out in the vertical direction. The molecular adsorption energy due to interaction with the surface drops roughly a factor of 10 going from the first to second layers, due to the short range of the surface potential, providing little driving force for order in layers beyond the first. Despite this *vertical* delocalization of the molecules in successive layers, the second layer does show well-localized *lateral* structure due mainly to van der Waals attractions of about −6 kcal/mol. Variations in vertical distance along an alkane chain are also observed with a pronounced deviation occurring in all layers near the chain ends. Experimental observation of fuzzy regions in the troughs between lamellae correlate well with the predictions of vertical motion at the ends of the surface adsorbed molecules as predicted by these MD simulations.

In this same study the motion of a single long chain of $C_{350}H_{702}$ on a graphite surface was studied using molecular dynamics.[93] Unlike the case of densely packed layers where entropy effects are very important, the predominant orientation of the carbon zigzag plane parallel to the graphite surface is thermally stable. Significant lateral motion on the surface is observed on the molecular dynamics time scale suggesting the need for low temperature or some form of chemical pinning to prevent sliding of the adsorbed species across the surface.

A simple model for dense phases of two dimensional hard rods has been used to study the packing of mono- and bidisperse systems confined to a plane.[94] Despite its simplicity, a number of interesting observations, confirmed by experiment, can be made using this model. In particular mixtures of long and short rods are found to be most stable when they phase separate into regions of short and long rods rather than forming interspersed mixtures. In both theory and STM experiments crystalline order is found for short particles, while for long particles a columnar phase with one dimensional order perpendicular to the particle's long axis is predicted and observed (for an alkane of formula $C_{192}H_{386}$). In the columnar phase considerable motion along the molecular axis is predicted, which leads to blurring of molecule ends and a loss of lamellar order.

In another molecular dynamics calculation employing an AMBER (assisted model building with energy refinement) force field, the adsorption of the normal alkane $C_{14}H_{30}$ from a benzene solution onto the basal plane of graphite has been simulated.[95] This study provides a particularly clear exposition of the various competing effects of solvent, surface−alkane interactions, and alkane−alkane interactions. The alkane chains diffusing within the range of the surface potential are found to penetrate the highly structured benzene layers near the surface and adhere to the graphite. The adsorbed chains strongly favor stretched conformations with mean square end-to-end separations equal to about 90% of that predicted by an all trans conformation of $C_{14}H_{30}$. Long-chain molecules introduced into the bulk of the sample take approximately 200 ps to spread uniformly throughout the solution eventually settling on the graphite and displacing the benzene molecules. The ability of the alkanes to displace benzene appears to be explained by the fact that the alkane is more stable on the surface by −0.18 kcal/(Å^2 mol) than the benzene. Though this particular simulation consisted of only seven alkane molecules in a benzene solution, some tendency for the alkane chains to order parallel to each other was observed at the longest time scales studied (1.3 ns). The plane of the zigzag chain of the alkane carbon atoms was found to adsorb parallel to the graphite surface as opposed to the perpendicular orientation found for chains in a dense monolayer where lateral interchain interactions dominate the energetics and entropy of the interfacial layer orientation.

Experimental and molecular dynamics studies of alkanes C_nH_{2n+2}, with $n = 16$, 17, 20, 28, and 32 have also been made.[96] In this study the molecular dynamics calculations simulated the adsorption of molecules from the gas phase onto graphite surfaces. MD simulations of the adsorption of single molecules of hexadecane and dotriacontane on graphite were performed. Gas-phase hexadecane molecules far from the surface undergo considerable fluctuations in length that are found to damp upon adsorption on the graphite surface. The adsorption step is complete within 200 ps, and the molecules are found to straighten and stiffen on the surface remaining extended for long periods of time. The molecular axis along the zigzag carbon backbone plane lies nearly parallel to the graphite surface. The carbon atoms in the alkane chain are not found to be in registry with the lattice but tend to occupy sites in which each methylene unit has one carbon atom close to a saddle point of the graphite carbon−carbon bond while the second carbon sits near to the center of the ring.

The molecular dynamics approach has been extended to the study of mixtures of benzene and 1,12-dodecanediol adsorbed on graphite surfaces, providing the first such study of a long-chain molecule with a functional end group.[98] Of particular interest is the fact that the well-pronounced ordering of the benzene molecules adjacent to the graphite surface (observed in the absence of alkyl solute) is lacking when the surface is covered by an alkyl monolayer. The mobility of the benzenes transverse to the surface is reduced adjacent to a bare graphite surface compared to a covered one. Hydrogen bonds between the diol molecules lead to an interconnection between neighboring lamella, with OH···O groups forming these bonds in an almost linear config-

uration. Because these diols have an even number of backbone atoms, the two ends of the molecule have OH groups that point away from or toward the graphite substrate at opposite ends, assuming the molecule adsorbs with its zigzag carbon backbone perpendicular to the surface. MD simulations show that the OH group pointing away from the surface has an almost equal probability of being trans or gauche, suggesting that dynamical features may be relatively easy to observe in these systems. It might also be expected that different contrast will be observed in the STM depending on the relative orientation of the OH group.

A calculation of the monolayer structure of dotriacontane on $MoSe_2$ has been performed using energy minimizations of periodic clusters of the alkane.[97] For the calculations solvent is not included, while the experimental STM studies were carried out for solutions of $C_{32}H_{66}$ adsorbed from the organic solvent phenyloctane on a $MoSe_2$ surface. Almost all of the surface adsorption energy is found to be due to the first two lattice planes consisting of Se and Mo with two-thirds of the energy coming from the first Mo plane. The corrugation of the $MoSe_2$ surface is considerably greater than on graphite and the adsorption energy is found to be roughly 2.5 kcal/mol compared to about 1.7 kcal/mol found for an analogous calculation on graphite. STM images show a contrast modulation along the lamellae having a periodicity extending over a little less than three molecules. The simulations indicate that this contrast modulation can be understood in terms of a modulation of the adsorbate−substrate separation. Thus, despite a number of approximations, good agreement is found between the experimentally observed and simulated images.

Molecular evaporation, condensation and crystallization of liquid *n*-alkane films (C_nH_{2n+2}, $n = 16-17$) on a Au(001) surface have also been studied using MD simulations methods.[99−101] Here it was found that the surface affects the crystallization of the alkane. The first four layers in a crystalline film of alkane molecules on Au(001) were found to orient parallel to the surface in a stretched conformation. Above the fourth layer molecules tended to orient parallel to the surface normal in the solid. These findings are consistent with the MD data obtained for liquid $C_{24}H_{50}$ on graphite in the absence of solvent, where the first layer of $C_{24}H_{50}$ was found to be parallel to the surface while successive layers are more and more smeared out in the vertical directions.[93]

IV.B. Experimental Observations of Dynamics at the Liquid−Solid Interface. Experimental observations of molecular motion can be obtained with the STM even in UHV environments[102,103] once the shape and orientation of a molecule on the surface can be distinguished, assuming the motion is slow enough to be observed on the STM time scale. The presence of solvent at the liquid−solid interface, of course, has a significant effect on the motion of dissolved molecules desorbing from and adsorbing to a surface. Some of the earliest studies of dynamic motion at the liquid−solid interface were made using a fast-scanning STM that permits observation of dynamic processes on a time scale of roughly 10 ms.[104,105] Dialkyl-substituted benzenes were imaged on graphite establishing the feasibility of STM studies on a number of functional groups by using long-chain alkyls to immobilize them on graphite. Both the benzene groups, which appeared bright in the STM images, and the alkyl side chains could be observed in these experiments. Sharp domain boundaries as well as defects in packing structure were observed and found to change slowly with time in these two-dimensional layered interface structures. The motion of the domain boundaries was ascribed to "free volume" diffusion. The motion of a domain boundary should be approximately energy neutral. In the case of the dialkylbenzenes, STM images indicate that the domains move by a rotation of the molecule about its long axis and a lateral displacement of the molecule by half its length. At least 12 molecules were found to move cooperatively to achieve the boundary shifts. Diffusion of defects within a lamella was also observed in this study.[105]

Variable-temperature STM was used to study molecular dynamics near an order-disorder transition in alkane monolayers at the interface between graphite and an organic solution.[106] Both melts and concentrated solutions were investigated for the molecules $C_{24}H_{50}$, $C_{32}H_{66}$, and $C_{192}H_{386}$ in phenyloctane. This work established the potential of the STM to study anisotropic molecular dynamics for order−disorder transitions at interfaces, identifying crystalline, smectic, and columnar phases in a single investigation. A temperature-dependent study of the *n*-alkanes (C_nH_{2n+2}, $n = 17-27$), in which loss of order was observed at high temperatures, has also been interpreted as providing evidence for order−disorder transitions on graphite surfaces.[107,108]

A particularly intriguing study of dynamic processes on surfaces has been performed with the alkane $C_{30}H_{62}$ on graphite.[51] Here a molten drop of the alkane wax was deposited on a horizontal surface, allowed to sit for several hours, and then quenched to room temperature. The surface was imaged several millimeters away from the edge of the drop using the STM in an attempt to observe the precursor layer surrounding a drop of a wetting molecular fluid. The precursor layer was successfully imaged about a millimeter from the edge of the solidified drop and the precursor layer found to be columnar with molecules extended and oriented along a graphite axis without any clean delineation of chain ends. Molecular image contrast varied from scan to scan suggesting molecular mobility of the precursor layer. Such columnar phases are usually only observed with much longer molecules or in binary mixtures. The observation of such a columnar phase indicates that the molecular density within this layer is smaller than at the solid−liquid interface for concentrated solutions of the same material.

Ordered monolayers of neat dodecanol have been studied on graphite at 303, 308, and 313 K, 6−36 K above the bulk melting temperature of 297 K.[109] Two distinct orderings of the adsorbed monolayer are observed. A herringbone structure is found at 303 and 308 K, while at 313 K the order mimics that found in the crystal with molecules in successive lamellae forming straight lines. The authors speculate that the transition to the higher temperature phase takes place via a rotator phase in which the molecules rotate about their C−O axes due to increased thermal energy. The phase transitions are reversible upon lowering the temperature. A similar explanation has been put forward to describe the presence of two different STM images observed in monolayers of Br atom terminated alkanes on graphite.[46]

Another variable-temperature study of long-chain molecules on graphite has been made using a novel quenching technique to freeze in high-temperature structures, which are then studied at lower temperatures.[110] The results of this study indicate that as the temperature increases, small longitudinal fluctuations of the molecules around their average position take place. Large-amplitude motion occurs at higher temperature along the molecular axis until the lamellae finally lose their identity through lateral disorder. While low-temperature phases show some resemblance with 3D smectic phases, the high-temperature phase is quite close to a nematic one, since longitudinal order is destroyed and only some degree of orientational order is retained.

Interconversion of two different 2D crystal structures of 2-hexadecylanthraquinone has been observed in a study of a number of anthrone derivatives adsorbed on graphite under phenyloctane solution.[111] These are molecules containing long alkane chains with aromatic groups attached to the ends. A number of these species were studied, but only the 2-hexadecylanthraquinone exhibited two coexisting crystal structures with lamella spacing differing by 50%. The simultaneous existence of two structures has been attributed to nucleation growth kinetics in which two nearly equal-energy structures form from the liquid phase. After several hours at room temperature only one of these forms persists. Oscillating structures have also been proposed to explain the more open of these two crystalline forms, with the oscillation being the result of a cooperative sliding movement of molecules parallel to one of the graphite main axes.

An interesting theoretical treatment of "noise" in STM experiments has been formulated in which the fluctuations in current are related to molecular motion in the region between surface and tip.[112] The idea is simply that the motion of adatoms in the tunneling gap will cause fluctuations in the barrier leading to a modulation of the tunnel current. If these fluctuations can be distinguished from "real noise" associated with mechanical and electronic fluctuations of the apparatus, it should be possible to retrieve information about molecular motion on the surface by Fourier decomposing the tunnel current. Although the characteristic frequencies for diffusion are in the range of 10^5 s^{-1} and experimentally accessible to the STM, the frequencies of molecular rotation are in the range 10^9-10^{12} s^{-1}. Considerable development in the frequency response of these instruments will be required before such high frequency motions will be detectable using STM methods.

In a study of chemical reaction dynamics occurring at the liquid−solid interface by STM, the oxidation of xanthine (a biologically important purine) has been studied in real time by imaging both the reactants and the products.[113] This study was carried out in water solvent, which necessitated coating the tunneling tips with Apiezon wax to reduce the Faradaic current. Growth of xanthine monolayer films was observed and found to take several minutes to reach completion following injection of sample into the liquid drop on top of the graphite. Reaction was initiated electrochemically and formation of product uric acid observed. The differences in STM images for reactant and product, plus the fact that both are adsorbed onto the surface, allow the appearance of product to be observed directly. The reaction was found to start preferentially from defect sights on the graphite surface.

V. Summary

The enormous potential for the STM to contribute to the understanding of important problems in molecule−surface interactions and molecular structure determination will be realized only if techniques are developed which make the imaging of molecular adsorbates routine. To this end, it will be important to gain a better understanding of the adsorbate's contribution to the tunneling processes, which makes imaging molecules possible, and the extent to which small changes in an adsorbate's structure can be detected. By using the STM to perform systematic investigations of terminally substituted alkanes, synthetic polymers, and self-assembled monolayers, the work described in this review has begun to test the limits of this instrument and the factors that lead to the successful imaging of molecular adsorbates. In addition, the application of the STM to these systems has also revealed details of molecule−surface interactions and molecule−molecule interactions, as well as their role in molecular epitaxy and the formation of two-dimensional crystal structures. Thus, we expect the research described here to contribute both to the development of STM techniques for observing adsorbed molecules and to our understanding of the physical interactions between molecules and between the surface and the adsorbates.

Acknowledgment. We are indebted to our colleagues in the scientific community for communicating their results to us, in many cases well before publication. Special thanks goes to our collaborators Professor Brian Bent, Professor George Whitesides, and Mr. Andrew Black for their help and encouragement in our own STM work. Work described here and performed at Columbia University was supported by the Joint Services Electronics Program (U.S. Army, Navy, and Air Force; DAAHO4-94-G0057), by National Institute of Health, PHS Grant 1 R03 RR06987-01A1, by the Donors of the Petroleum Research Fund administered by the American Chemical Society, and by the American Association of University Women.

References

(1) Tersoff, J.; Hamann, D. R. *Phys. Rev. B.* **1985**, *31*, 805.
(2) Rohrer, H. *Proc. Natl. Acad. Sci. U.S.A.* **1987**, *84*, 4666.
(3) Hamers, R. *Annu. Rev. Phys. Chem.* **1989**, *40*, 531.
(4) Binnig, G.; Rohrer, H.; Gerger, C.; Weibel, E. *Phys. Rev. Lett.* **1982**, *49*, 57.
(5) Mizutani, W.; Shigeno, M.; Sakakibara, Y.; Kajimura, K.; Ono, M.; Tanishima, S.; Ohno, K.; Toshima, N. *J. Vac. Sci. Tecnnol.* **1990**, *A8*, 675.
(6) Foster, J.; Frommer, J. *Nature* **1988**, *333*, 542.
(7) Smith, D.; Hörber, H.; Gerber, C.; Binning, G. *Science* **1989**, *245*, 43.
(8) Smith, D.; Heckl, W. *Nature* **1990**, *346*, 616.
(9) Smith, D. P. E.; Hörber, J. K. H.; Binning, G.; Nejoh, H. *Nature* **1990**, *344*, 641.
(10) Hara, M.; Iwakabe, Y.; Tochigi, K.; Sasabe, H.; Garito, A. F.; Yamada, A. *Nature* **1990**, 228.
(11) Iwakabe, Y.; Hara, M.; Kondo, K.; Tochigi, K.; Mukoh, A.; Yamada, A.; Garito, A.; Sasabe, H. *Jpn. J. Appl. Phys.* **1991**, *30*, 2542.
(12) McMaster, T.; Carr, H.; Miles, M.; Cairns, P.; Morris, V. *Macromolecules* **1991**, *24*, 1428.
(13) Breen, J. J.; Flynn, G. W. *J. Phys. Chem.* **1992**, *96*, 6825.
(14) Heckl, W.; Smith, D.; Binning, G.; Klagges, H.; Hänsch, T.; Maddocks, J. *Proc. Natl. Acad. Sci. U.S.A.* **1991**, *88*, 8003.
(15) Walba, D. M.; Stevens, F.; Parks, D.; Clark, N.; Wand, M. *Science* **1995**, *267*, 1144.

(16) Brandow, S. L.; Harrison, J. A.; DiLella, D. P.; Colton, R. J.; Pfeiffer, S.; Shashidhar, R. *Liquid Cryst.* **1993**, *13*, 163.
(17) Sleator, T.; Tycko, R. *Phys. Rev. Lett.* **1988**, *60*, 1418.
(18) Yang, R.; Naoi, K.; Evans, D.; Smyrl, W.; Hendrickson, W. *Langmuir* **1991**, *7*, 556.
(19) Quivy, A.; Deltour, R.; Bentum, P. J. M. v.; Gerritsen, J. W.; Jansen, A. G. M.; Wyder, P. *Surf. Sci.* **1995**, *325*, 185.
(20) Quint, P.; Knoll, W.; Hara, M.; Sasabe, H.; Duran, R. S. *Macromolecules* **1995**, *28*, 4029.
(21) Kimura, M.; Okumura, A.; Miyamura, K.; Gohshi, Y. *Jpn. J. Appl. Phys.* **1995**, *34*, 3642.
(22) Cornelison, D. M. *Surf. Sci.* **1995**, *343*, 87.
(23) Ara-Kato, N.; Yase, K.; Shigekawa, H.; Yoshimura, M.; Kawazu, A. *Synth.. Met.* **1995**, *70*, 1245.
(24) Bar, G.; Maganov, S. N.; Liang, W.; Whangbo, M.-H. *Synth. Met.* **1995**, 189.
(25) Wu, X.; Parakka, J. P.; Cava, M. P.; Kim, Y.-T.; Metzger, R. M. *Synth. Met.* **1995**, *71*, 2105.
(26) Frommer, J. *Angew. Chem., Int. Ed. Engl.* **1992**, *31*, 1298.
(27) Magonov, S. N.; Whangbo, M.-H. *Surface Analysis with STM and AFM: experimental and theoretical aspects of image analysis*; VCH Publishers: New York, 1996.
(28) Groszek, A. J. *J. Proc. R. Soc. London* **1970**, *314*, 473.
(29) Findenegg, G. H. *J. Chem. Soc., Faraday Trans.* **1972**, *68*, 1799.
(30) Findenegg, G. H. *J. Chem. Soc., Faraday Trans.* **1973**, *69*, 1069.
(31) Rabe, J. P.; Buchholz, S.; Askadskaya, L. *Synth. Met.* **1993**, *54*, 339.
(32) McGonigal, G. C.; Bernhadt, R. H.; Thomson, D. J. *Appl. Phys. Lett.* **1990**, *57*, 28.
(33) Abrahamsson, S.; Larson, G.; Sydow, E. V. *Acta Cyrstallogr.* **1960**, *13*, 770.
(34) Rabe, J. P.; Buchholz, S. *Science* **1991**, *253*, 424.
(35) Venkataraman, B.; Breen, J. J.; Flynn, G. W. *J. Phys. Chem.* **1995**, *99*, 6608.
(36) McGonigal, G. C.; Bernhadt, R. H.; Yeo, Y. H.; Thomson, D. J. *J. Vac. Sci. Technol.* **1991**, *B9(2)*, 1107.
(37) Watel, G.; Thibaudau, F.; Cousty, J. *Surf. Sci.* **1993**, *281*, L297.
(38) Liang, W.; Whangbo, M.-H.; Wawkuschewski, A.; Cantow, H. J.; Magonov, S. N. *Adv. Mater.* **1993**, *5*, 817.
(39) Venkataraman, B.; Flynn, G. W., unpublished results.
(40) Hibino, M.; Sumi, A.; Hatta, I. *Jpn. J. Appl. Phys.* **1995**, *34*, 3354.
(41) Cartmell, E.; Fowles, G. W. A. *Valency and Molecular Structure*, 3rd ed.; D. Van Nostrand Co.: Princeton, NJ, 1966.
(42) Venkataraman, B.; Flynn, G. W.; Wilbur, J.; Folkers, J. P.; Whitesides, G. M. *J. Phys. Chem.* **1995**, *99*, 8684.
(43) Porter, M. D.; Bright, T. B.; Allara, D. L.; Chidsey, C. E. D. *J. Am. Chem. Soc.* **1987**, *109*, 3559.
(44) Laibinis, P. E.; Whitesides, G. M.; Allara, D. L.; Tao, Y.-T.; Parikh, A. N.; Nuzzo, R. G. *J. Am. Chem. Soc.* **1991**, *113*, 7152.
(45) Cyr, D. M.; Flynn, G. W., unpublished results.
(46) Cyr, D. M.; Venkataraman, B.; Flynn, G. W.; Black, A.; Whitesides, G. M. *J. Phys. Chem.*, in press.
(47) Stabel, A.; Dasaradhi, L.; O'Hagan, D.; Rabe, J. P. *Langmuir* **1995**, *11*, 1427.
(48) Wawkuschewski, A.; Cantow, H.-J.; Magonov, S. N.; Möller, M.; Liang, W.; Whangbo, M.-H. *Adv. Mater.* **1993**, *5*, 821.
(49) Wawkuschewski, A.; Cantow, H.-J.; Magonov, S. N. *Langmuir* **1993**, *9*, 2778.
(50) Magonov, S. N.; Wawkuschewski, A.; Cantow, H.-J.; Liang, W.; Whangbo, M.-H. *Appl. Phys.* **1994**, *59*, 119.
(51) Askadskaya, L.; Boeffel, C.; Rabe, J. P. *Ber. Bunsen-Ges. Phys. Chem.* **1993**, *97*, 517.
(52) Liu, T.-L.; Parakka, J. P.; Cava, M. P.; Kim, Y.-T. *Synth. Met.* **1995**, *71*, 1989.
(53) Cincotti, S.; Rabe, J. P. *Appl. Phys. Lett.* **1993**, *62*, 3531.
(54) Elbel, N.; Günther, E.; Seggern, H. v. *Appl. Phys. Lett.* **1994**, *65*, 642.
(55) Welland, M. *Phys. World* **1994**, 32.
(56) Manne, S.; Gaub, H. E. *Science* **1995**, *270*, 1480.
(57) Ueno, N.; Fukushima, T.; Sugita, K.; Kiyono, S.; Seki, K.; Inokuchi *J. Phys. Soc. Jpn.* **1980**, *48*, 1254.
(58) Wandelt, K.; Jacob, W.; Memmel, N. d. *Phys. Rev. Lett.* **1986**, *57*, 1643.
(59) Eigler, D. M.; Weiss, P. S.; Schweizer, E. K.; Lang, N. D. *Phys. Rev. Lett.* **1991**, *66*, 1189.
(60) Demuth, J. E.; Avouris, P.; Schmesser, D. *Phys. Rev. Lett.* **1983**, *50*, 600.
(61) Ukraintsev, V. A.; Long, T. J.; Harrison, I. *J. Chem. Phys.* **1992**, *96*, 3957.
(62) Ukraintsev, V. A.; Long, T. J.; Gowl, T.; Harrison, I. *J. Chem. Phys* **1992**, *96*, 9114.
(63) Patrick, D.; Beebe, T. P., Jr. *Langmuir* **1994**, *10*, 298.
(64) Hallmark, V. M.; Chiang, S.; Meinhardt, K.-P.; Hafner, K. *Phys. Rev. Lett.* **1993**, *70*, 3740.
(65) Biscarini, F.; Bustamante, C.; Kenkre, V. M. *Phys. Rev. B.* **1995**, *51(16)*, 11089.
(66) Chen, C. J. *Scanning Microsc.* **1993**, *7*, 793.
(67) Fisher, A. J.; Blöchl, P. E. *Phys. Rev. Lett.* **1993**, *70*, 3263.
(68) Kenkre, V. M.; Biscarini, F.; Bustamante, C. *Phys. Rev. B* **1995**, *51*, 11074.
(69) Lindsay, S. M.; Sankey, O. F.; Li, Y.; C., H.; Rupprecht, A. *J. Phys. Chem.* **1990**, *94*, 4655.
(70) Lindsay, S. M.; Li, Y.; Pan, J.; Thundat, T.; Nagahara, L. A.; Oden, P.; DeRose, J. A.; U. K. *J. Vac. Sci. Technol. B* **1991**, *9*, 1096.
(71) Lindsay, S. M.; Lyubchenko, Y. L.; Tao, N. J.; Li, Y. Q.; Oden, P. I.; DeRose, J. A.; Pan, J. *J. Vac. Sci. Technol. A* **1993**, *11(4)*, 808.
(72) Mintmire, J. W.; Harrison, J. A.; Colton, R. J.; White, C. T. *J. Vac. Sci. Technol. A.* **1992**, *10(4)*, 603.
(73) Mujica, V.; Kemp, M.; Ratner, M. A. *J. Chem. Phys.* **1994**, *101*, 6849.
(74) Mujica, V.; Kemp, M.; Ratner, M. A. *J. Chem. Phys.* **1994**, *101*, 6856.
(75) Nejoh, H. *Appl. Phys. Lett.* **1990**, *57*, 2907.
(76) Schmickler, W. *J. Electroanal. Chem.* **1990**, *269*, 283.
(77) Spong, J. K.; Mizes, H. A.; LaComb Jr, L. J.; Dovek, M. M.; Frommer, J. E.; Foster, J. S. *Nature* **1989**, *338*, 137.
(78) Somorjai, G. A. *Introduction to Surface Chemistry and Catalysis*; Wiley-Interscience: New York, 1994.
(79) Mizutani, W.; Shigeno, M.; Ohmi, M.; Suginoya, M.; Kajimura, K.; Ono, M. *J. Vac. Sci. Technol. B* **1991**, *9*, 1102.
(80) Mizutani, W.; Shigeno, M.; Ono, M.; Kajimura, K. *Appl. Phys. Lett.* **1990**, *56(20)*, 1974.
(81) Thibaudau, R.; Watel, G.; Cousty, J. *Surf. Sci. Lett.* **1993**, *281*, L303.
(82) Sautet, P.; Bocquet, M.-L. *Surf. Sci. Lett.* **1994**, *304*, 445.
(83) Sautet, P.; Dunphy, J. C.; Ogletree, D. F.; Joachim, C.; Salmeron, M. *Surf. Sci.* **1994**, *315*.
(84) Smith, D. P. E. *J. Vac. Sci. Technol. B* **1991**, *9*, 1119.
(85) Rivera, M.; Williamson, R. L.; Miles, M. J. *J. Vac. Sci. Technol. B* **1996**, *14*, 1472.
(86) Yackoboski, K.; Yeo, Y. H.; McGonigal, G. C.; Thomson, D. J. *Ultramicroscopy* **1992**, *42−44*, 963.
(87) Kobayashi, M. *J. Chem. Phys.* **1978**, *68*, 145.
(88) McClure, D. W. *J. Chem. Phys.* **1968**, *49*, 1830.
(89) Jarrett, W. L.; Mathias, L. J.; Alamo, R. G.; Mandelkern, L.; Dorset, D. L. *Macromolecules* **1992**, *25*, 3468.
(90) Sirota, E. B.; Jr., H. E. K.; Shao, H. H.; Singer, D. M. *J. Phys. Chem.* **1995**, *99*, 798.
(91) Meyer, A. Y. *Tetrahedron* **1975**, *31*, 1971.
(92) Momany, F. A.; Bonham, R. A.; McCoy, W. H. *J. Am. Chem. Soc.* **1963**, *85*, 3077.
(93) Hentschke, R.; Schürmann, B. L.; Rabe, J. P. *J. Chem. Phys.* **1992**, *96*, 6213.
(94) Hentschke, R.; Askadskaya, L.; Rabe, J. P. *J. Chem. Phys.* **1992**, *97*, 6901.
(95) Hentschke, R.; Winkler, R. G. *J. Chem. Phys.* **1993**, *99*, 5528.
(96) Lupkowski, M.; Maguire, J. F. *Composite Interfaces* **1994**, *2*, 1.
(97) Cincotti, S.; Burda, J.; Hentschke, R.; Rabe, J. P. *Phys. Rev. E* **1995**, *51*, 2090.
(98) Winkler, R. G.; Hentschke, R. *J. Chem. Phys.* **1994**, *100*, 3930.
(99) Xia, T. K.; Landman, U. *J. Chem. Phys.* **1994**, *101*, 2498.
(100) Xia, T. K.; Landman, U. *Phys. Rev. B* **1993**, *48*, 11313.
(101) Ribarsky, M. W.; Landman, U. *J. Chem. Phys.* **1992**, *97*, 1937.
(102) Hallmark, V. M.; Chiang, S.; Brown, J. K.; Wöll, C. *Phys. Rev. Lett.* **1991**, *66*, 48.
(103) Chiang, S.; Hallmark, V. M. *J. Vac. Sci. Technol. B* **1994**, *12*, 1957.
(104) Buchholz, S.; Rabe, J. P. *J. Vac. Sci. Technol. B* **1991**, *9*, 1126.
(105) Rabe, J. P.; Buchholz, S. *Phys. Rev. Lett.* **1991**, *66*, 2096.
(106) Askadskaya, L.; Rabe, J. P. *Phys. Rev. Lett.* **1992**, *69*, 1395.
(107) Couto, M. S.; Liu, X. Y.; Meekes, H.; Bennema, P. *J. Appl. Phys.* **1994**, *75*, 627.
(108) Michel, B.; Travaglini, G.; Rohrer, H.; Joachim, C.; Amrein, M. *Z. Phys. B* **1989**, *76*, 99.
(109) Yeo, Y. H.; McGonigal, G. C.; Thomson, D. J. *Langmuir* **1993**, *9*, 649
(110) Bucher, J.-P.; Roeder, H.; Kern, K. *Surf. Sci.* **1993**, *289*, 370.
(111) Stabel, A.; Heinz, R.; Rabe, J. P.; Wegner, G.; Schryver, F. C. D.; Corens, D.; Dehaen, W.; Süling, C. *J. Phys. Chem.* **1995**, *99*, 8690.
(112) Kornyshev, A. A. *J. Electroanal. Chem.* **1994**, *376*, 9.
(113) Tao, N. J.; Shi, Z. *Surf. Sci.* **1994**, *321*, L148.

CM960113A